For
Submitted to
Nature 10/86

STRUCTURAL AND HYDROLOGIC FRAMEWORK OF THE NORTHERN BARBADOS RIDGE COMPLEX: RESULTS OF LEG 110 ODP

J. Casey Moore
Department of Earth Sciences
University of California at Santa Cruz
Santa Cruz, CA 95064, U.S.A.

Alain Mascle
Institut Francais du Petrole
1-4 Ave. Bois-Preau
B.P. 311
92506 Rueil Malmaison Cedex, France

Elliott Taylor
Ocean Drillling Program
Texas A & M University
College Station, TX 77843-3469, U.S.A.

Patrick Andreieff
BRGM
BP 6009
45060 Orleans Cedex-2, France

Francis Alvarez
Borehole Research Group
Lamont Doherty Geological Observatory
Columbia University
Palisades, NY 10964, U.S.A.

Ross Barnes
Rosario Geoscience Associates
104 Harbor Lane
Anacortes, WA 98221, U.S.A.

Christian Beck
Departement des Sciences de la Terre
Universite de Lille
59655 Villeneuve d'Ascq Cedex, France

Jan Behrmann
Institut fuer Geowissenschaften und Lithosphärenforschung
Universitaet Giessen
Senckenbergstr. 3
D6300 Giessen, Fed. Rep. of Germany

Gerard Blanc
Laboratorie de Geochimie
Universite Pierre et Marie Curie
4 Place Jussieu
75252 Paris Cedex 05, France

Kevin Brown
Department of Geological Sciences
Durham University
South Road
Durham, DH1 3LE, England

Murlene Clark
Department of Geology
LSCB 341
University of South Alabama
Mobile, AL 36688, U.S.A.

James Dolan
Earth Sciences Board
University of California at Santa Cruz
Santa Cruz, CA 95064, U.S.A.

Andrew Fisher
Division of Marine Geology and Geophysics
University of Miami
4600 Rickenbacker Causeway
Miami, FL 33149, U.S.A.

Joris Gieskes
Ocean Research Division A-015
Scripps Institution of Oceanography
La Jolla, CA 92093, U.S.A.

Mark Hounslow
Department of Geology
Beaumont Building
Sheffield University
Brook Hill
Sheffield, SE 7HF, England

Patrick McClellan
Petro-Canada Resources
P.O. Box 2844
Calgary, Alberta, Canada

Kate Moran
Atlantic Geoscience Centre
Bedford Institute of Oceanography
Box 1006
Dartmouth, Nova Scotia B2Y 4A2, Canada

Yujiro Ogawa
Department of Geology
Faculty of Science
Kyushu University 33
Hakozaki, Fukuoka 812, Japan

Toyosaburo Sakai
Department of Geology
Faculty of General Education
Utsunomiya University
350 Mine-machi
Utsunomiya 321, Japan

Jane Schoonmaker
Hawaii Institute of Geophysics
2525 Correa Road
Honolulu, HI 96822, U.S.A.

Peter J. Vrolijk
Earth Sciences Board
University of California at Santa Cruz
Santa Cruz, CA 95064, U.S.A.

Roy Wilkens
Earth Resources Laboratory
E34-404 M.I.T.
Cambridge, MA 02139, U.S.A.

Colin Williams
Borehole Research Group
Lamont-Doherty Geological Observatory
Columbia University
Palisades, NY 10964, U.S.A.

SUMMARY

Leg 110 of the Ocean Drilling Project cored through the fault between the Caribbean plate and the underthrusting Atlantic oceanic crust, achieving a first-ever penetration of a detachment surface or decollement zone separating two plates in a subduction zone. Pore water chemistry, temperature anomalies, and

structural observations indicate that the deforming sediments dewater through fracture permeability associated with faults and that the accretionary wedge and underthrust sediments comprise separate fluid domains separated by a permeability barrier above the decollement zone. Methane-bearing fluids derived from a probable thermogenic source travel more than 25 km beneath the shallowly inclined decollement.

INTRODUCTION

Subduction zones are the most dynamic tectonic environment on earth providing insights into the very beginning of the mountain building process. Subduction zones consume water-rich sediment that evolves to highly deformed rock of negligible porosity, requiring large-scale fluid expulsion (1). The consequent fluid flow and attendant high fluid pressures influence many aspects of subduction zone geology, including the shape of the accretionary wedge (2), thrust faulting and fold vergence (3, 4), heat transport (5), diagenesis and metamorphism (6), and benthic biology (7). Analysis of the origin, migration, and sediment interactions of fluids is therefore critical to unraveling the complicated and dynamic history of subduction zones.

The subduction zone hydrogeology is best studied in modern active systems. As drilling provides an effective tool for probing this dynamic environment, Leg 110 of the Ocean Drilling Project (ODP) was designed to investigate structural, hydrologic, and diagenetic effects of the transition from undeformed deep sea

sediment to stratally disrupted melange in a subduction zone separating the Caribbean plate and the Atlantic oceanic crust.

The Barbados Ridge, the eastern boundary of the Caribbean plate, is a wide accretionary complex associated with the Lesser Antilles volcanic arc. The Barbados Ridge formed in the last 45 my by offscraping of sediment riding on the subducting Atlantic ocean crust (8, 9). The northern portion of the Barbados Ridge complex became the focus of subduction zone drilling because the sedimentary cover of the incoming oceanic crust is less than 800 m thick; consequently the decollement surface and related thrust faults occur at relatively shallow depths below the seafloor. Previous drilling during Leg 78A of the Deep Sea Drilling Project (DSDP) documented thrust faulting by biostratigraphic repetition in the accretionary wedge, discovered indications of high fluid pressures in the decollement, but failed to penetrate this major fault surface (10).

STRUCTURAL FRAMEWORK OF THE LEG 110 TRANSECT

The prime objective of Leg 110, penetrating the decollement, was realized at our first drillsite, Site 671 (Figs. 1,2), a surprising result in view of former attempts to drill this mechanically unstable zone at the same location on DSDP Leg 78A. At Site 671 we cored 500 m of Pleistocene to lower Miocene imbricately thrusted offscraped calcareous mud and mudstone, a 40 m thick decollement zone of lower Miocene to upper Oligocene scaly (sheared and flattened) mudstone, and 150 m of slightly deformed underthrust Oligocene mudstone, marlstone and siltstone (Fig. 3). Although we drilled well into the underthrust sequence,

the hole had to be terminated above the oceanic crust due to penetration of an unstable sand layer. ODP Sites 671, 675, and 676, as well as DSDP Sites 541 and 542, all located near the deformation front, provided excellent control on the geometry of the imbricate packages (Fig 2). Good biostratigraphy permitted unequivocal recognition of thrust faults and provided a basis for correlation between all holes drilled during ODP Leg 110 and DSDP Leg 78A.

In order to understand the development of the structural fabrics, physical properties, and water chemistry in subduction zone, we drilled a reference hole at Site 672, 6 km east of the deformation front along the the Leg 110 site transect. Here we defined the characteristics of all units penetrated in the accretionary wedge in a relatively undisturbed state. A distinctive lithology and excellent fossil control at the top of the decollement zone allowed identification of correlative strata at the reference site. Anomalously high porosity and probably correlative decrease in sediment strength characterize this "future decollement" and could explain why failure initiates at this stratigraphic level. Indeed, low- angle shear zones, and normal and reverse faults suggest incipient failure, even at this substantial distance seaward of the deformation front. A methane anomaly near the level of the "future decollement" suggests, furthermore, that fluid may be advecting laterally at this level. Because of enhanced cementation the middle to upper Eocene sandy interval which stopped drilling at Site 671 was completely penetrated at the reference site. Low chloride and relatively

high methane contents in pore water from sandy layers likewise suggest lateral fluid flow from beneath the accretionary wedge. Thus, even at 6 km to the east of the deformation front Site 672 appears to show some effects of the encroaching accretionary wedge. About 10 km east of the deformation front of the Southern Barbados Ridge complex a mud volcano may also be generated by lateral movement of fluid from the subduction zones (11).

In addition to documenting initial accretionary history, Leg 110 drilled Sites 673 and 674, west and 12 and 17 km up slope, respectively, of the deformation front, to measure the continuing evolution of the offscraped sediments. Sedimentary rocks cored at these two sites were far more complexly deformed than in sites near the deformation front. Deformation features such as overturned sections, scaly fabrics, stratal disruption, veining and cataclastic shear zones are similar to those occurring in subaerially exposed accretionary complexes (e.g. Barbados Island, 12, 13). More remarkably, this intensity of deformation was achieved with only modest dewatering, resulting in sedimentary deposits with about fifty percent porosity. Lastly, we were able to define thrust packages with relatively coherent internal stratigraphy near the deformation front; similar tectonic units at Sites 673 and 674 are cut by later thrusts that are discordant to their complexly evolving interiors. Moreover, the landward-dipping seismic reflectors here appear to correlate with these later thrusts, not the internal stratigraphy of the tectonic units.

HYDROLOGIC FRAMEWORK

A combination of structural, biostratigraphic, seismic, and physical property data clearly define a structural setting within which the the hydrologic evolution of the Leg 110 transect can be considered. Any model of the hydrogeology of the accretionary wedge must account for sources of fluids, mode of transport, and the geometry of the conduits.

The average porosity of sedimentary deposits at the reference Site 672 is about 54%. Decrease in average porosities of sites located at the deformation front and further up slope are not dramatic. Comparisons of particular stratigraphic intervals do, however, document localized fluid loss. The modest dewatering of the offscraped sequence appears to occur principally in response to vertical, as opposed to lateral, tectonic loading. The underthrust portion of the incoming sediment, although undeformed, is progressively loaded by the westward thickening accretionary wedge which would undoubtedly result in consolidation, overpressure, and water loss.

Sedimentary deposits in the Leg 110 area are dominantly fine-grained and of low permeability (14), with the exception of the locally sandy interval in the underthrust sequence. The geochemical evidence presented below argues for dewatering in the decollement zone. However, a simple calculation using Darcy's law shows that fluid movement through the intergranular permeability of the ubiquitous fine-grained sediments would be about one thousand times slower than the rate of underthrusting.

Hence, water cannot escape up the decollement zone unless the permeability here is increased by fractures. Supporting this argument, the foliated decollement zone includes rhodochrosite-filled veins in the scaly fabric suggesting that Site 675 fluid pressures were sufficiently high to allow opening these surfaces for fluid flow. We surmise that flow through the fine-grained sediments of the accretionary wedge and decollement zone is dominated by fracture permeability, especially along faults. In contrast, the middle and upper Eocene sandy deposits of the underthrust section (Fig. 3) probably transport fluid by intergranular flow through the permeable sands.

Chemistry of the pore water provides the most clear-cut evidence for fluid movement along faults and to a lesser degree stratigraphic conduits. Many faults penetrated during Leg 110 included waters with low chloride contents (Fig. 4). Apparently these low chloride values are caused by movement of fluid through a clay membrane which preferentially retains salts on the high pressure side (15, 16). Accordingly, the faults are not only surfaces of fluid movement but must have, at times, a lower fluid potential than the surrounding sediments which are their fluid sources. The low chloride contents noted just above the sandy interval at Site 671 (Fig. 4) and within the same sequence at Site 672 suggest lateral flow along this permeable horizon. Because the observed pore water anomalies would diffusively decay in 1 to 2 x 10^5 years (17) they must represent active fluid flow. Anomalously high concentrations of methane occur in pore waters within the decollement zone, in adjacent faults, and the sandy

interval below the decollement. However, no methane anomalies are recognized in faults in the accretionary wedge more than a few tens of meters above the top of the decollement zone, even though these surfaces display low chloride values indicating flow (Fig. 4). The accretionary wedge and underthrust sediment appear to constitute discrete fluid domains separated by the top of the decollement zone.

Rather than due to membrane filtration, the low chloride waters observed in the Leg 110 cores could be due to the decomposition of methane hydrate, as occurs in the slope sediments of the Middle America Trench (18,19). However, no hydrate reflectors appear in any of the seismic lines in the Leg 110 area. Moreover, low chloride values occur both with and without associated methane. Hydrate decomposition produces both methane and low chloride water.

Temperature data provide additional evidence supporting the geochemical arguments for fluid flow. High temperature gradients (76 to 180°C/km) were measured at shallow levels at each site predicting unreasonably high temperatures at depth. At Site 674 where measurements were extended to several hundred meters sub-bottom, a near-surface gradient of 143°C/km decreased to a more normal value of 28°C/km (Fig. 4), suggesting that the high surface gradients are explained by lateral input along faults. In fact, at Site 674 a change in temperature gradient, a negative anomaly in chloride, and a probable fault nearly coincide, provide evidence of lateral flow of warm, low chloride fluids along fracture permeability. A similar correlation of an increased

temperature gradient up-section with a porewater geochemical anomaly occurs also at Site 676 in the vicinity of the frontal thrust.

Methane at and below the decollement zone is probably not biogenically produced in situ because of the locally high sulphate concentrations (20). Instead, this hydrocarbon is most likely advected through the underthrust sediment from beneath the accretionary wedge. Since methane is not present in the upper levels of the accretionary wedge, it is not being produced biogenically here, notwithstanding low sulfate concentrations. Because the background geothermal gradient is less than 30°C/km at Site 674 and the accretionary wedge here is less than 2 km thick, methane is probably not generated thermogenically in adjacent accreted materials. Sediment below the decollement is deeply underthrust and would ultimately reach a depth of thermogenic methane generation (21) west of Site 674, suggesting that the methane observed at Sites 671, 672, and 675 has advected more than 25 km laterally. Methane may also be more prevalant below the decollement because the sediments now being underthrust are slightly richer in organic matter than those being offscraped (0.1 versus 0.14 % total organic carbon, respectively).

Fluid expulsion along fault zones indicates that they are locally and periodically regions of low fluid potential (pressure), relative to the source beds. Yet, to undergo continued movement, the fault zones must also be weaker than the adjacent sediments. Perhaps the cohesion and internal friction of the sediments in the faults is sufficiently lower than the

surrounding sediment to obviate any differences in pore pressure (22). Alternatively, displacement and fluid flow may occur in separate portions of fault zones with locally variable fluid pressure (23). Finally, displacement and fluid expulsion may be part of complex cyclical pattern of fault activity and occur at differing times.

From a simple geometric perspective, fluids exiting from below the decollement should flow vertically to the sea floor rather than laterally along the shallowly inclined decollement. Material just over the decollement zone must present a permeability barrier to vertical flow. The preference for lateral flow may reflect the higher fracture permeability of prominent scaly fabric along the decollement zone. Any permeability barrier over the decollement zone may, in part, be caused by the expected change in stress orientation across the top of the decollement zone (Fig. 2B). The low plunge of the maximum principal stress in the accretionary wedge (Fig. 2A) would discourage opening of steeply dipping fractures by high fluid pressure while encouraging flow along shallowly dipping surfaces.

CONCLUSIONS

Seismic data and drilling results from near the deformation front in the Leg 110 area indicate that the Neogene oceanic sedimentary section is imbricately offscraped with the subjacent Paleogene and Cretaceous sedimentary deposits being underthrust with the oceanic crust beneath a well defined seismic decollement. Twelve to seventeen kilometers up-slope of the

deformation front the offscraped sediment packages continue to be internally deformed and are cut by prominent late thrusts that correlate with landward dipping reflections on seismic profiles. The accretionary wedge and much of the underthrust section is dominated by fine-grained, low permeability sedimentary deposits. Fluid escape must occur primarily through zones of enhanced fracture permeability, commonly associated with faults, and secondarily along stratigraphically controlled zones of higher intergranular permeability. Geochemical and temperature anomalies indicate fluid movement along faults. Fluid expulsion along fault zones indicates that they must locally have lower fluid potential (pressure) than the adjacent source sediment. Pore water chemistry specifies two major fluid domains: the accretionary wedge produces fluid with low chloride content and no methane; fluids sampled adjacent to or below the decollement yield low chloride water with significant methane contents. The top of the decollement zone represents a permeability barrier constraining fluid to flow laterally below it. Overall, our results indicate significant lateral movement of fluids in a subduction zone with associated advection of solutes and heat transport.

FIGURE CAPTIONS

1) Location map showing the setting of the eastern boundary of the Caribbean plate and the Atlantic abyssal plain (inset) as well as a generalized Seabeam map with locations of the sites drilled during ODP Leg 110 and DSDP Leg 78A, and the network of seismic reflection lines.

2) Cross sections showing the structural and hydrologic framework of the Leg 110 area. A) Structural framework of the Leg 110 area based on a depth-section constructed from seismic line CRV 128 and all drilling results. At the deformation front offscraped sediment is imbricately stacked along young thrust faults; up-slope these faults and the deformed internal stratigraphy of the initial imbricate packages are cut by late thrust faults with an orientation similar to the early imbricate thrusts. B) Hydrologic framework of Leg 110 area. Arrows show directions of fluid flow. In the accretionary wedge, methane-free, low-chloride fluids are most conspicuous along faults at Sites 673 and 674, representing the evolving dewatering of the wedge. Along the Leg 110 site transect, methane is only sourced below the decollement as the underthrust sediments are carried to levels of thermogenic methane generation; methane-bearing fluids could also be expected in the accretionary wedge farther west as it thickens. Insets show state of stress in accretionary wedge and in oceanic sediment column well removed from disturbing effects of deformation front (24). Because of decoupling below the decollement zone, the orientation of stress in the underthrust undeformed sediments should differ significantly from that in the overthrust accretionary wedge, and perhaps is more similar to their initial state on the oceanic crust.

3) Lithologic columns and structural features from ODP Leg 110 and DSDP Leg 78A sites. Note transition along level of decollement zone from incipient structures at Site 672 to

well developed scaly fabric zone at Site 671. Moreover, overall intensity of scaly fabrics and faulting increases from east to west upslope in offscraped material.

4) Relationship of structural features, pore water chemistry, and temperature gradient. Low chloride high and methane porewater concentration at Site 671 correlate with both the decollement zone and top of a permeable sand horizon, and characterize the methane-bearing fluid regime. At Site 674 many, but not all faults correlate with lows in the chloride curve, suggesting some faults may be active conduits of fluid transport. The overall low chloride values probably reflect a diffusive decrease of this constituent due to long-term flow of fluids through this highly faulted section. Correlation of the chloride low with the change in temperature gradient at 30 to 40 m sub-bottom at Site 674 suggests currently active flow. Note that methane is absent along all faults in the accretionary wedge at Site 674, characterizing the methane-free fluid domain. A small methane anomaly just above the decollement at Site 671 suggests minor leakage through this permeability barrier.

REFERENCES

1. Bray, C. J. and Karig, D. E. J. Geophys. Res. v. 90, p. 768-778 (1985).

2. Davis, D., J. Suppe, and F.A. Dahlen. J. Geophys. Res. v. 88, p. 1153-1172 (1983).

3. Hubbert, M. K. and W. W. Rubey. Geol. Soc. Am. Bull. v. 70, p. 115-166 (1959).

4. Seely, D.R. In Talwani, M., and Pitmann, S.C., (eds.), Island Arcs, Deep Sea Trenches, and Back-Arc Basins, Am. Geophys. Union Maurice Ewing Series 1, p. 187-198 (1977).

5. Langseth, M. G. and Hobart, M. A. EOS v. 65, p. 1089 (1984).

6. Etheridge, M. A., Wall, V. J., and Vernon, R. H. Jour. Metamorphic Geol. v. 1, p. 205-226 (1983).

7. Kulm, L. D., Suess, E., Moore, J. C., Carson, B., Lewis, B. T., Ritger, S. D., Kadko, D. C., Thornberg, T. M., Embley, R. W., Rugh, W. D., Massoth, G. J., Langseth, M. G., Cochran, G. R., and Scamman, R. L. Science v. 231, p. 561-566 (1986).

8. Westbrook, G., Mascle, A., and Biju-Duval, B. In Biju-Duval, B., Moore, J. C., et al., Init. Repts. DSDP v. 78A: Washington (U.S. Government Printing Office), p. 23-38 (1984).

9. Bouysse, P. in Biju-Duval, B., Moore, J.C. et al., Init. Repts. DSDP, 78A: Washington (U.S. Govt. Printing Office) p. 83-102 (1984).

10. Biju-Duval, B., Moore, J. C., et al. v. 78A: Washington (U. S. Government Printing Office), 621 p (1984).

11. Westbrook, G. K. and Smith, M. J. Geology v. 11, p. 279-283 (1983).

12. Speed, R. C. and Larue, D. K. J. Geophys. Res. v. 87, p. 3633-3643 (1982).

13. Mascle, A., Biju-Duval, B., de Clarens, P. and Munsch, H. in Wezel, D. (ed.), The Origin of Arcs: Elsevier Sci. Pub. Co. in press).

14. Marlow, M. S., Lee, H., and Wright, A. In Biju-Duval, B., and Moore J. C., et al., Init. Repts. DSDP v. 78A: Washington, D.C., (U.S. Government Printing Office), p. 549-558 (1984).

15. Freeze, R. A., and Cherry, J. A. Prentice-Hall Inc. (Englewood Cliffs, N.J.) 604 p (1979).

16. Kharaka, Y.K., Hull, R.W. and Carothers, W.W. in Relationship of Organic Matter and Mineral Diagene sis: Soc. Econ. Paleon. and Min., Short Course no. 17, p. 79-174 (1985).

17. Gieskes, J.M. Ann. Rev. Earth Planet. Sci. v. 3, p. 433-453 (1975).

18. Hesse, R., Lebel, J. and Gieskes, J.M. in von Huene, R., Aubouin, J. et al., Init. Repts. DSDP. 84: Washington (U.S. Govt. Printing Office) p. 727-736 (1984).

19. Gieskes, J.M., Johnston, K. and Boehm, M. in von Huene, R., Aubouin, J. et al., Init. Repts. DSDP, 84: Washington (U.S. Govt. Printing Office) p. 961-967 (1984).

20. Claypool, G. E., and Kaplan, I. R. In: Kaplan, I. R. (Ed.), Natural gases in marine sediments v. 3, Plenum Press, New York, p. 99-139 (1974).

21. Waples, D.W. Intl. Human Resources Development Corp., Boston 232 p. (1985).

22. Lambe, T. W., and Whitman, R. V. John Wiley and Sons, Inc., New York 553 p (1969).

23. Karig, D. E. in: J. C. Moore ed., Synthesis of Structural Fabrics from DSDP Cores from Forearcs, Geol. Soc. Am. Memoir in press (1986).

24. Davis, D. M. In Biju-Duval, B., Moore, J. C. et al., Init. Repts. DSDP v. 78A: Washington (U.S. Govt. Printing Office), p. 569-579 (1984).

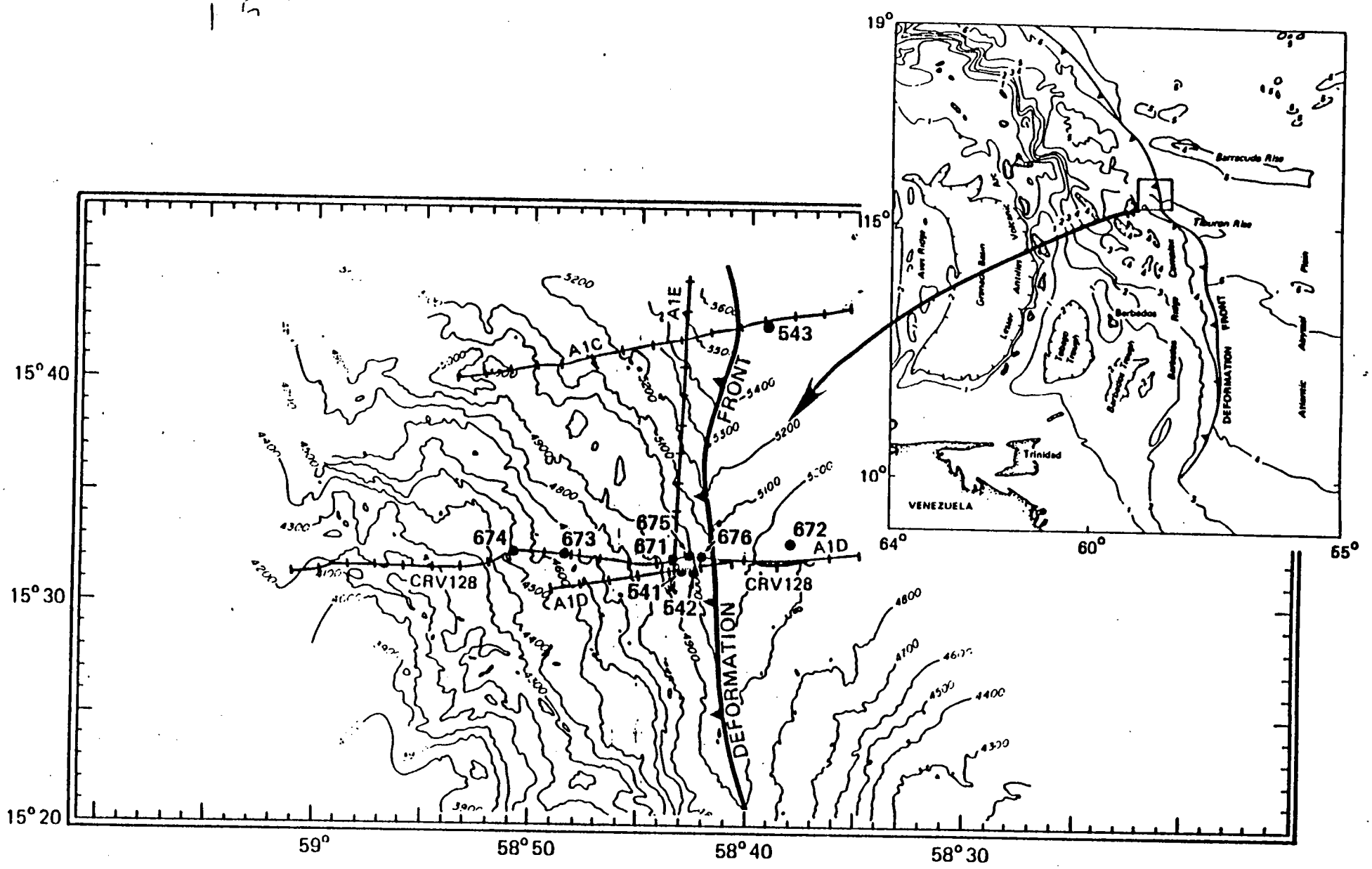
19°
15°
10°
64°
60°
55°
Barracuda Rise
Tiburon Rise
Barbados
DEFORMATION FRONT
Trinidad
VENEZUELA
15°40
15°30
15°20
59°
58°50
58°40
58°30
A1E
A1C
A1D
CRV128
543
675
674
673
671
676
672
541
542
FRONT
DEFORMATION

Fig 1

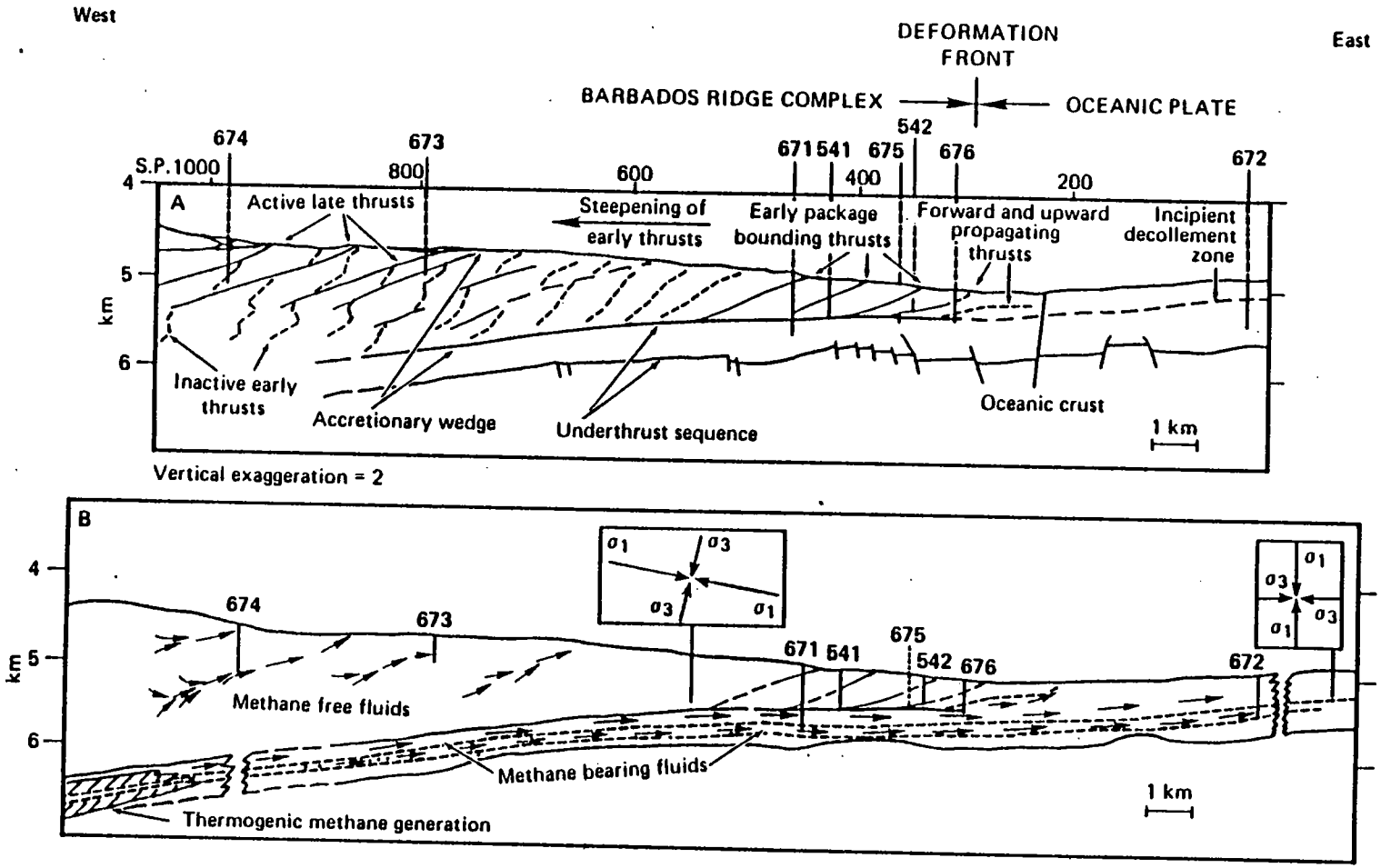
West
East
DEFORMATION FRONT
BARBADOS RIDGE COMPLEX
OCEANIC PLATE
674
673
671
541
542
675
676
672
S.P. 1000
800
600
400
200
A
Active late thrusts
Steepening of early thrusts
Early package bounding thrusts
Forward and upward propagating thrusts
Incipient decollement zone
km
4
5
6
Inactive early thrusts
Accretionary wedge
Underthrust sequence
Oceanic crust
1 km
Vertical exaggeration = 2
B
σ_1
σ_3
Methane free fluids
Methane bearing fluids
Thermogenic methane generation

Fig 2

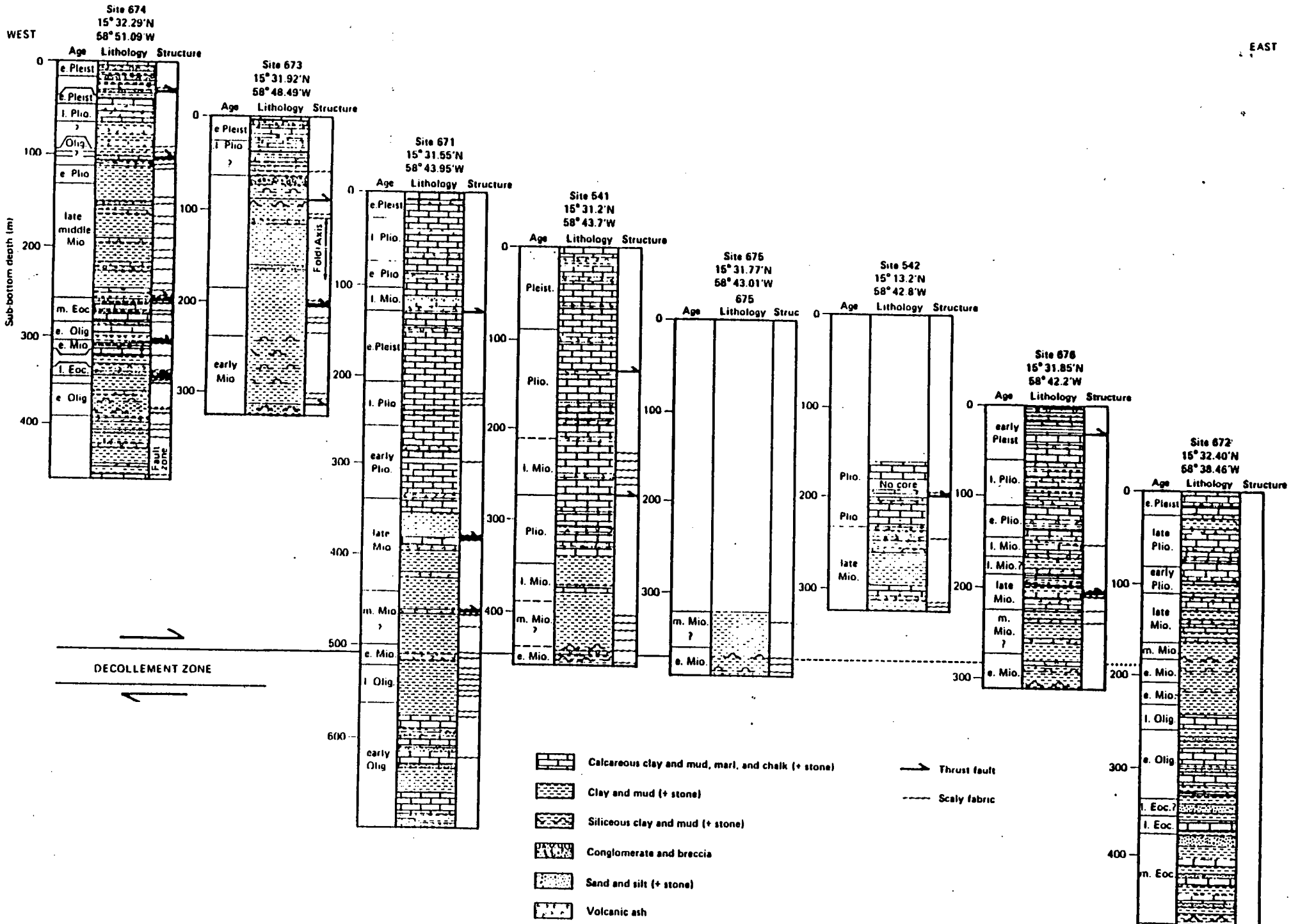
WEST
EAST
Sub-bottom depth (m)
Site 674
15°32.29'N
58°51.09'W
Site 673
15°31.92'N
58°48.49'W
Site 671
15°31.55'N
58°43.95'W
Site 541
15°31.2'N
58°43.7'W
Site 675
15°31.77'N
58°43.01'W
Site 542
15°13.2'N
58°42.8'W
Site 676
15°31.85'N
58°42.2'W
Site 672
15°32.40'N
58°38.46'W
Age
Lithology
Structure
e. Pleist
l. Plio.
Olig.
e. Plio
late middle Mio
m. Eoc
e. Olig
e. Mio
l. Eoc.
e Olig
Fault zone
Fold Axis
early Mio
e.Pleist
l. Plio.
e. Plio
l. Mio.
early Plio.
late Mio
m. Mio
e. Mio.
l. Olig.
early Olig
Pleist.
Plio.
m. Mio.
No core
late Mio.
early Pleist
e. Plio.
l. Mio.
l. Mio.?
m. Mio.?
late Plio.
e. Eoc.
DECOLLEMENT ZONE
Calcareous clay and mud, marl, and chalk (+ stone)
Clay and mud (+ stone)
Siliceous clay and mud (+ stone)
Conglomerate and breccia
Sand and silt (+ stone)
Volcanic ash
Thrust fault
Scaly fabric

Fig 3

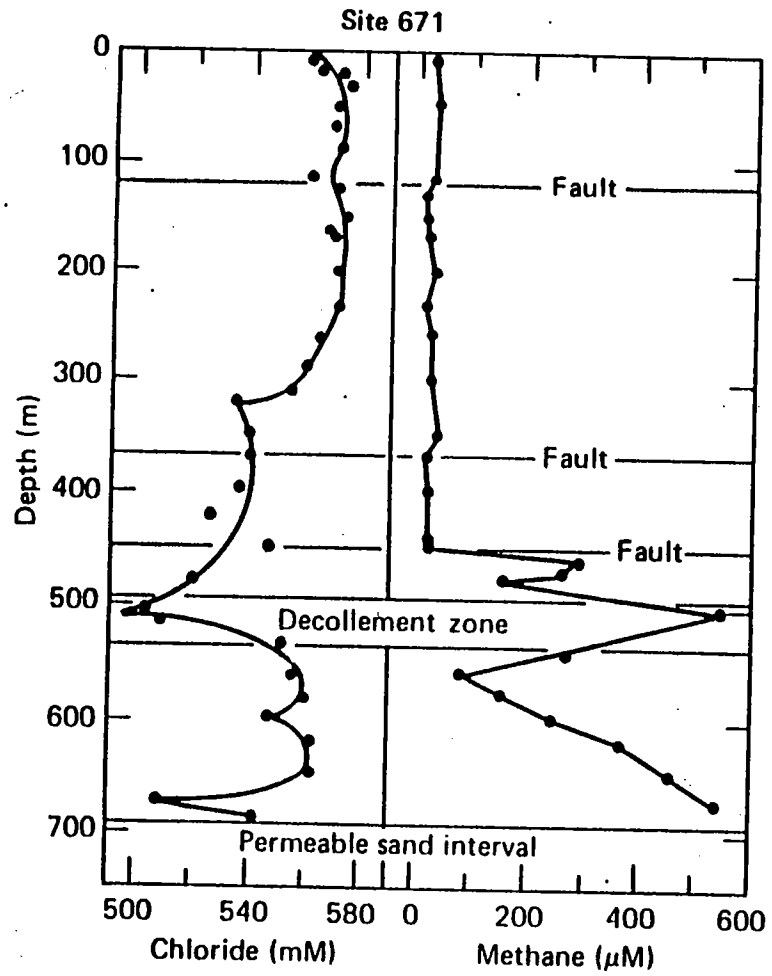
Site 671
Depth (m)
0
100
200
300
400
500
600
700
Fault
Fault
Fault
Decollement zone
Permeable sand interval
500
540
580
Chloride (mM)
0
200
400
600
Methane (μM)

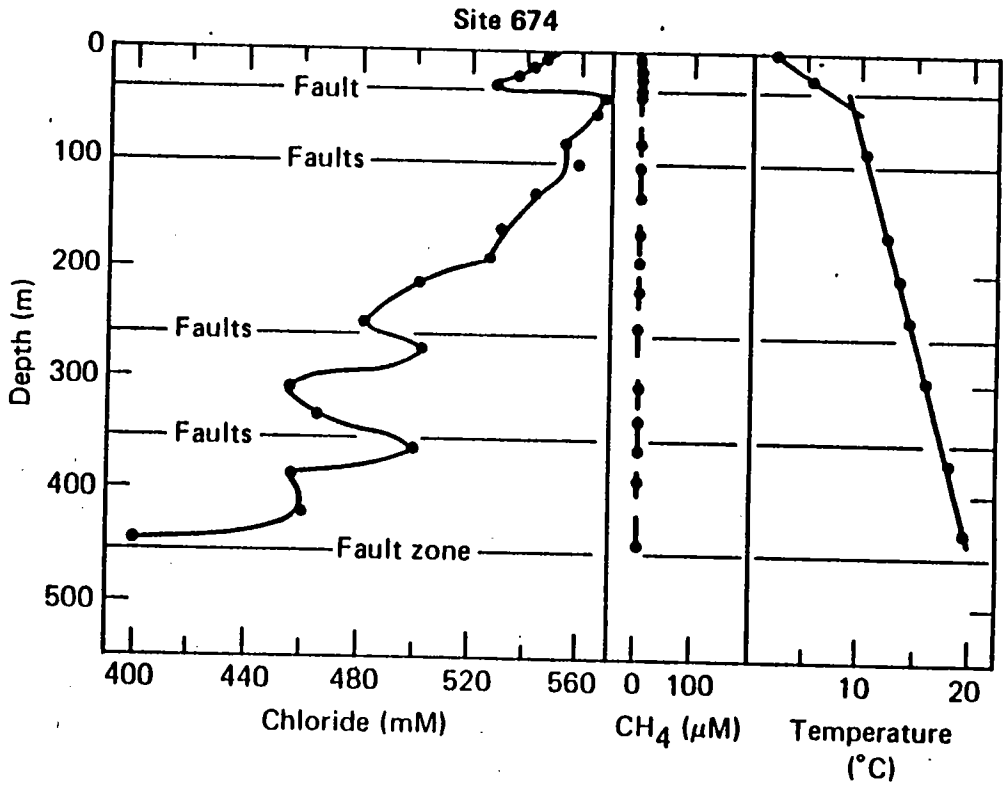
Site 674
Depth (m)
0
100
200
300
400
500
Fault
Faults
Faults
Faults
Fault zone
400
440
480
520
560
Chloride (mM)
0
100
CH4 (μM)
10
20
Temperature (°C)

Fig 4